

Spatial and Temporal Properties of Neurons of the Lateral Suprasylvian Cortex of the Cat

M. CONCETTA MORRONE, MARIROSA DI STEFANO, AND DAVID C. BURR

Department of Psychology, University of Western Australia, Nedlands, Western Australia 6009

SUMMARY AND CONCLUSIONS

1. Neurons in the posteromedial lateral suprasylvian cortex (PMLS) of cats were recorded extracellularly to investigate their response to stimulation by bars and by sinusoidal gratings.

2. Two general types of cells were identified: those that modulated in synchrony with the passage of drifting bars and gratings and those that responded with an unmodulated increase in discharge. Both types responded to contrast reversed gratings with a modulation of activity: the cells that modulated to drifting gratings modulated to the first harmonic of contrast reversed gratings (at appropriate spatial phase and frequency), whereas those that did not modulate to drifting gratings always modulated to the second harmonic of contrast reversed gratings. No cell had a clear null point.

3. Nearly all cells were selective for spatial frequency. The preferred frequency ranged from 0.1 to 1 cycles per degree (cpd), and selectivity bandwidths (full width at half height) were around two octaves. Preferred spatial frequency was not correlated with receptive field size, but bandwidth and receptive field size were positively correlated. Preferred spatial frequency decreased with eccentricity, at about 0.05 octaves/deg.

4. The response of all cells increased as a function of grating contrast up to a saturation level. The contrast threshold for response to a grating of optimal parameters was $\sim 1\%$ for most cells and the saturation contrast $\sim 10\%$. The contrast gain was ~ 25 spikes/s per log unit of contrast.

5. All cells were tuned for temporal frequency, preferring frequencies from ~ 3 to 10

Hz, with a selectivity bandwidth ~ 2 octaves. For some cells, the spatial selectivity did not depend on the temporal frequency and vice versa. Others were spatiotemporally coupled, with the preferred temporal frequency being lower at high than at low spatial frequencies, and the preferred spatial frequency lower at high than at low temporal frequencies. Previous results showing broad velocity tuning to a bar were replicated and found to be predictable from the combined spatial and temporal tuning of PMLS cells and the Fourier spectrum of a bar. Preferred temporal frequency steadily decreased with eccentricity, at 0.025 octaves/deg.

6. The results for PMLS cells are compared with those of other visual areas. Acuity and spatial preference and selectivity bandwidth is comparable to all areas except *area 17*, where they are a factor of about two higher. Temporal selectivity in PMLS is as fine as observed in other areas. The possibility that PMLS cells may be involved with motion detection and detection of motion in depth is discussed.

INTRODUCTION

The lateral suprasylvian visual cortex (LS or area of Clare-Bishop) is a large and important part of the cat's visual system. It receives direct thalamic afferents from the medial interlaminar nucleus (MIN) and C laminae of the dorsal lateral geniculate body and lateral posterior-pulvinar complex nucleus of the thalamus (7, 30, 35, 38, 52, 62, 64). It also receives afferents from cortical areas 17, 18, and 19 (from both sides), as well as from the contralateral LS (8, 54). It can be considered, therefore, as a point of convergence of the

genicular-cortical and fugal visual pathways.

The area of LS most studied is the post-medial area (PMLS) (49). PMLS cells have very large receptive fields, often with a substantial ipsilateral projection and are usually binocularly driven (15, 33, 43, 49, 58, 69). The fields have no distinct on-off regions, but inhibitory flanks outside the receptive field have been described (15, 33). Cells are broadly tuned for orientation, but most have a preferred direction of motion (33, 58). They are said to respond well to moving stimuli over a wide range of velocities, but not to flashed stimuli (15, 29, 58, 66). Despite the large extent of PMLS receptive fields, they have quite high-spatial acuity [2 cycles per degree (cpd) at best], about the same as all visual areas except *area 17* (23).

To understand better the possible role the lateral suprasylvian areas play in vision, we investigated in detail the spatial and temporal properties of LS neurons. We did so using the now well-established technique of stimulation by sinusoidal gratings of variable spatial frequency, temporal frequency, and contrast. This technique has yielded fruitful results in various visual areas from retina to cortex in various species (3, 11, 16, 24, 32, 37, 39, 40, 44, 45, 46, 53).

METHODS

Preparation

Experiments were performed on 12 intact adult cats. The cats were initially anaesthetized with ketamine hydrochloride (Ketalar 10 mg/Kg, im) for incanulation of a femoral vein, and then anaesthetized with thiopental sodium (Pentothal, 1–2 ml, 2.5% solution iv). A small patch of skull and dura was removed for electrode insertion. Wounds and pressure points were treated with long lasting local anesthetic (Anocaine). During recording the animal was paralyzed (pancuronium bromide, 0.2–0.3 ml · kg⁻¹ · h⁻¹, iv) and artificially ventilated with N₂/O₂ (70:30%). End-tidal respiratory CO₂ was kept constant at 3.5–4%, and body temperature, electroencephalogram (EEG), and electrocardiogram (ECG) were constantly monitored. Small doses of thiopental were infused as needed to maintain slow-wave activity of the EEG (28).

The corneas were protected with contact lenses (3-mm artificial pupil) and refraction corrected to 57 cm. The position of the vertical meridian and area centralis was determined by the standard techniques of optic disk projection (9, 34).

Electrode penetrations were made along the medial wall of the medial suprasylvian sulcus. The electrode was angled medially 25–35° from the vertical between A6 and APO stereotaxic coordinates, which define the area of PMLS (49). The electrodes were glass micropipettes (1 μm tip), filled with NaCl electrolyte. Electrical potentials were suitably amplified, filtered and pulse shaped, then led into both an auditory amplifier and a computer (Digital PDP-11/10).

For five cats the recording electrode was filled with pontamine in sodium acetate (0.5 M) that was applied iontophoretically (10–20 μA) after each penetration. These animals were perfused at the end of the experiment. Brain slices, stained with neutral red, were examined microscopically for electrode reconstruction. The histology always confirmed that the recording electrode was positioned in PMLS.

Stimuli

For locating cells, mapping receptive fields, and determining ocular preference, hand-held stimuli (such as bars and dots) were projected onto a tangent screen 57 cm from the cat with an overhead projector. In general the most convenient stimuli proved to be dark bars against a bright screen (29).

After initial hand plotting of receptive field, the tangent screen was replaced with an oscilloscope (Joyce Electronics) that displayed drifting or flickering bars or sinusoidal gratings. The oscilloscope had a mean luminance of 50 cd/m² and subtended 30 × 30° at 57 cm. The gratings were produced by standard raster techniques (at 100 frames/s, 1,200 lines/frame) from waveforms generated by computer (Digital PDP-11/10). A rotatable yoke on the oscilloscope allowed the raster to be rotated mechanically to produce stimuli of appropriate orientation. Stimulus contrast was controlled by the computer by analogue multiplication.

The computer also recorded the cell spike train. During the oscilloscope flyback, it computed and displayed poststimulus time histograms. At the end of a data set, it calculated mean firing rate and amplitude of modulation, both at the fundamental frequency of the stimulus and at higher harmonics (by means of Fourier analysis). Cell response to gratings was taken either as the increase in mean firing rate with respect to the spontaneous discharge just prior to stimulation or as the amplitude of modulation at either the fundamental or second harmonic. Response to single bars was taken as the difference between peak response and spontaneous activity.

To determine response dependency on contrast, or spatial or temporal frequency, the computer program automatically varied the parameter systematically while recording the response. For example, to produce the contrast response curves of Fig. 9, the computer set the contrast to the lowest

desired level, displayed the grating stimulus and began to average the response. After 100 sums, it increased the contrast and recommenced summing. The procedure was repeated, contrast increasing up to the desired maximum. Between conditions, a measure was taken of the spontaneous discharge to provide a base line of cell activity, against which the response could be normalized. The whole process was then repeated, reversing the direction of contrast change. The same sort of procedure was used to scan spatial frequency and temporal frequency.

For important data, curve collection was often repeated several times during the life of the cell and several key points for each condition checked randomly. This meant that to obtain a complete and reliable set of data on all the variables that interested us would require that we held the cell for 12 h. In reality, it was possible to obtain complete curves on only two or three variables during the 3 or 4 h of cell life. Often, after excessive stimulation by optimal stimuli, a cell became difficult to stimulate reliably: some adapted, responding only weakly to all stimuli, whereas others showed excessive increase of spontaneous activity. On these occasions, we allowed the cell to rest for 20–30 min before continuing analysis.

RESULTS

Response to bars and gratings

Compared with cells from many other visual structures (such as LGN and cortical areas 17 and 18) PMLS cells are difficult to record from reliably. They have high and variable spontaneous activity, which increases after prolonged stimulation by high contrast stimuli. The response to stimuli is also variable and diminishes rapidly as the cell adapts. Many PMLS cells require binocular stimulation to elicit a strong response (4, 67). Our apparatus did not permit binocular stimulation (with appropriate alignment), and response to monocular stimulation was often too weak for detailed quantitative analysis. For these reasons, out of the 120 cells isolated, we were able to obtain quantitative data on only 57.

For all cells, the general procedure was to study first the receptive field properties, such as position, size, binocularity, orientation, and direction preference with hand-plotting techniques and then to collect poststimulus time histograms in response to stimulation by bars or gratings. Figure 1 shows the poststimulus

time histograms of two cells to stimulation by a drifting bar and by a drifting sinusoidal grating. Consider first the response to the bar. Cell *A* responded with a fairly homogeneous increase in mean firing rate. Cell *B*, however, responded with a modulated discharge that increased as the bar passed some regions and decreased as it passed others, reflecting subregions of opposite polarity in the receptive field. In response to sinusoidal gratings cell *A* responded with a homogeneous increase in mean firing rate, with no modulation of discharge. Cell *B* showed some overall increase in firing rate, but mainly a strong modulation of discharge in synchrony with the passage of grating bars. Cell *A* behaved like a complex cell of area 17 or 18 and cell *B* like a simple or simple-like cell of area 17 or 18 (21, 39, 44, 45).

To quantify better the different behavior of cells, we measured the ratio of the first harmonic modulation to the mean of the cell response for four or five of the optimal stimuli and then averaged the ratios to obtain a single value for each cell. This index of relative modulation (RMI) of response is closely related to the index used by De Valois et al. (22) in the study of the macaque visual cortex and by Dean and Tolhurst (21) for area 17 of the cat.

Figure 2 shows the distribution of the relative modulation of the response. The distribution has two peaks: one for modulation indexes < 0.2 and another for indexes between 0.8 and 1. Forty percent of the cells fall in the first peak (RMI < 0.2), implying weak or non-existent modulation. Thirty percent of the cells had RMI > 0.8 , implying that the modulation is a major feature of their response. The other 30% of cells had intermediate RMIs of 0.3–0.7. These cells usually modulated to only some particular stimuli and the modulation was accompanied with a pedestal increase in mean firing rate.

In general, it was easier to study the receptive field properties with gratings than with bars. The precise response of the cell to bars depended critically on many factors, such as the magnitude and sign of the contrast (they usually prefer black bars on a light background; 29), drift velocity (direction and speed), and bar width. Changing these variables can alter drastically the apparent size of the receptive field and the apparent positions of the regions of differential sensitivity. The

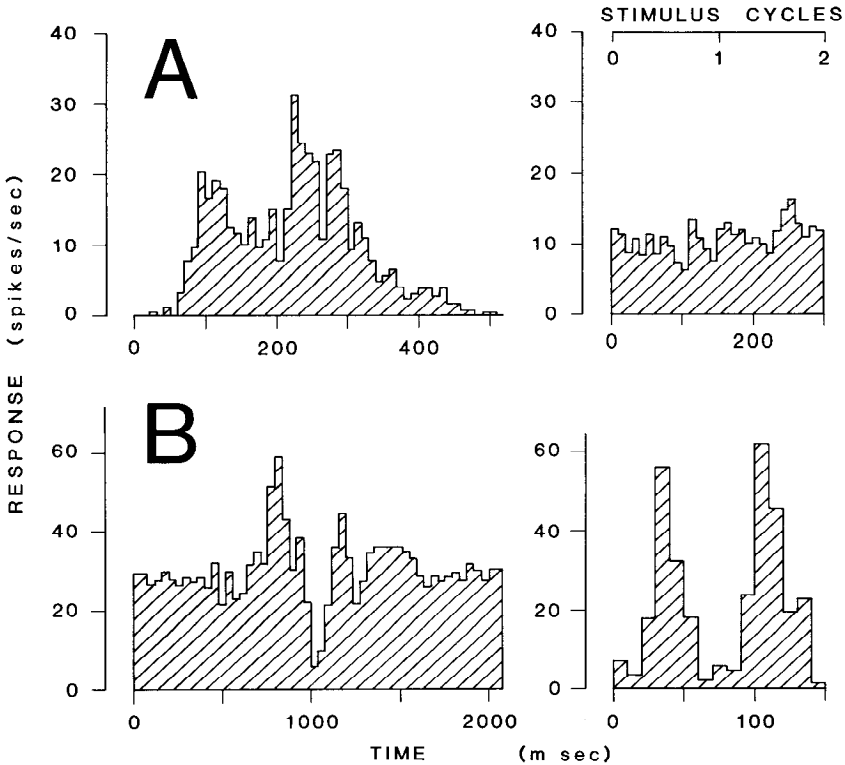


FIG. 1. Poststimulus time histograms for 2 representative cells (*A* and *B*) in response to drifting black bars (*left column*) and to drifting sinusoidal gratings (*right column*). Parameters for cell in *A*: bar width 2.5 deg, drift speed 50 deg/s; grating spatial frequency 0.2 cpd; temporal frequency 6.7 Hz (velocity 33.5 deg/s); contrast 8%; spontaneous activity 1.5 spikes/s. For cell in *B*: bar width 1 deg, drift speed 16 deg/s; grating spatial frequency was 0.8 cpd temporal frequency 13.3 Hz (velocity 16.6 deg/s); contrast 15%; spontaneous activity 15 spikes/s. Histograms are the average of 75 sums.

response to gratings tended to be far more robust over the range of variable parameters.

Flicker

Sinusoidal gratings caused to reverse periodically are a useful tool for classifying cell properties. They provide a strong test of linear summation of the receptive field (24, 55). Quasilinear cells (like retinal and geniculate X-cells and *area 17* simple cells) respond to flickering gratings at the same frequency as the flicker rate (1st harmonic modulation). By varying the position of the grating (spatial phase), a point can be found where the response vanishes (“null point”). Nonlinear cells (such as Y-cells, complex-cells, and simple-like cells of *area 18*), however, have no null point, and generally respond at twice the frequency of the flicker rate (second harmonic modulation), depending on spatial frequency and other parameters (24, 39, 55, 57, 59).

Figures 3 and 4 show the response of two types of PMLS cells to flickering gratings. The cell in Fig. 4 responded at twice the flicker frequency, irrespective of the frequency or phase of the stimulus grating. This is clear ev-

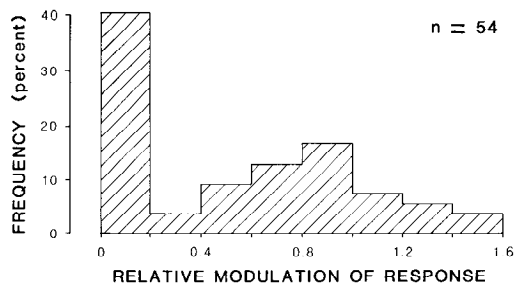


FIG. 2. Frequency distribution of the relative modulation index for 54 cells. Index is the average ratio of the first harmonic modulation to the increase in mean discharge, measured at 4 or 5 spatial frequencies.

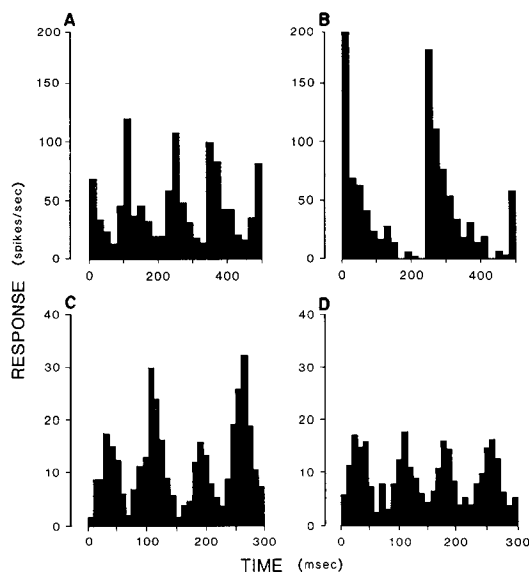


FIG. 3. Response of 2 separate cells to a stationary sinusoidal grating whose contrast is modulated sinusoidally over time. One cell is shown in the *top* of figure (*A* and *B*), the other in the *bottom* (*C* and *D*). *Left column* shows results for 1 spatial phase of the counter-phased grating, the *right* the response to the same grating shifted in phase by π . For cell of *A* and *B* spatial frequency was 0.36 cpd, temporal frequency 4 Hz, and contrast 30%. Cell acuity was 0.9. For cell *C* and *D* the spatial frequency was 0.5 cpd, temporal frequency 6.6 Hz, and contrast 35%. Cell acuity was 0.7 cpd. The poststimulus time histograms have been computed on 100 sums. At appropriate spatial phase both cells modulate to only the second harmonic (*A* and *D*). A phase shift of π causes a first harmonic component to appear in the modulation (*B* and *C*), particularly for cell response *B*.

idence of nonlinear summation of the receptive field. This cell had an on/off receptive field with no clear subregions and responded to drifting gratings with an unmodulated increase in discharge (like the cell in Fig. 1*A*; RMI = 0.03). In all these properties, this cell is similar to a classical cortical complex cell (45, 59).

The two cells in Fig. 3, however, could respond at either the fundamental or second harmonic frequency of the stimulus, depending on spatial phase of the grating. There was no clear null point, but at one phase the response had a strong component at the flicker frequency, and 90° from this the modulation was all at twice the flicker frequency. These cells also showed nonlinear summation, but the nonlinearity was of the type observed by Spitzer and Hochstein (59, 60) for interme-

diated and mixed complex cells, rather than for classical complex cells. These cells had a partially discrete receptive field organization, and responded with modulated discharge to drifting gratings (RMI = 1.3 and 0.9).

All the cells we measured behaved either like the two cells in Fig. 3 or that in Fig. 4. We found none with evidence of linear summation. Of our population, 40% modulated at twice the stimulus frequency irrespective of spatial phase and 60% depended on spatial phase. All those that only modulated to the second harmonic had RMIs < 0.2, and those that showed first harmonic modulation at some phases had RMIs between 0.4 and 1.3.

For some cells in our sample, we measured the spatial and temporal frequency selectivity using flickering as well as drifting gratings. The gratings were positioned to elicit maximum second harmonic response (if the response depended on position, like one cell on Fig. 3). For flicker as well as for motion (see next section), cells were highly selective to both temporal and spatial frequency. The tuning curves produced by the two methods were always similar (see for example Fig. 12*C*).

Spatial frequency selectivity

For 36 cells, we measured response as a function of grating spatial frequency. Figure 5 shows the results for four representative cells. Like cells in other cortical areas, each of these cells responded best to gratings of a specific spatial frequency. For frequencies above or below this optimum, the response was progressively weaker. That is to say, they behaved as spatial band-pass filters.

Figure 5 reports response as increase in mean firing rate, rather than as modulation amplitude (although two cells did modulate with RMI < 1). Figure 6 shows tuning curves for two additional cells, plotted both as increase in mean firing rate and first harmonic modulation amplitude. For the cell of Fig. 6*A* the curves were similar for the two measures. However, for the cell in Fig. 6*B* the modulation tuning curve is double peaked, whereas the mean increase curve is not. Seven other cells behaved like cell in Fig. 6*B*, with double-peaked modulation tuning curves. For two of these cells the optimum spatial frequency was different when measured with the two discharge parameters. The remaining four cells that modulated behaved like the cell in Fig.

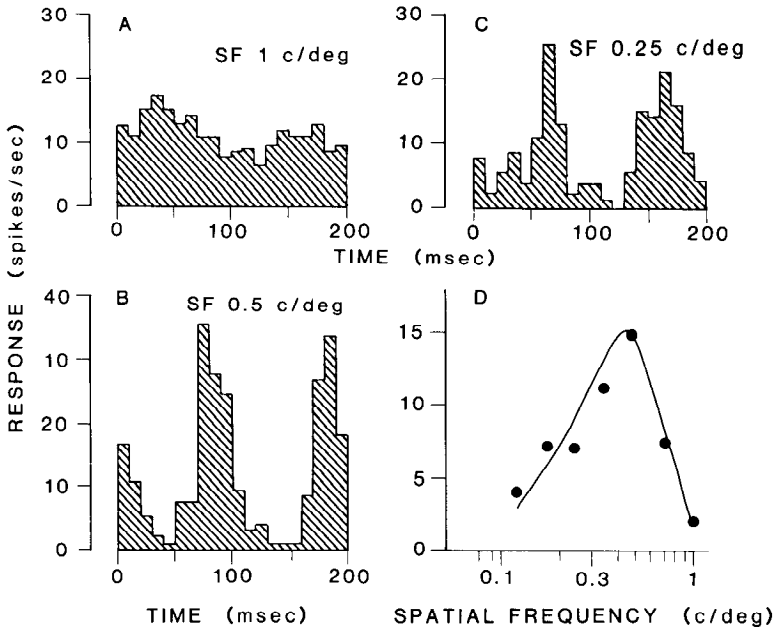


FIG. 4. *A, B, and C*: poststimulus time histograms of the response of a posteromedial lateral suprasylvian cortex cell to a contrast reversed grating for 3 different spatial frequencies. Temporal frequency was 5 Hz and the contrast 30%. Histograms have been calculated on 75 sums. *D*: amplitude of modulation on the second harmonic of the stimulus of the same cell as function of the spatial frequency of the contrast-reversed grating.

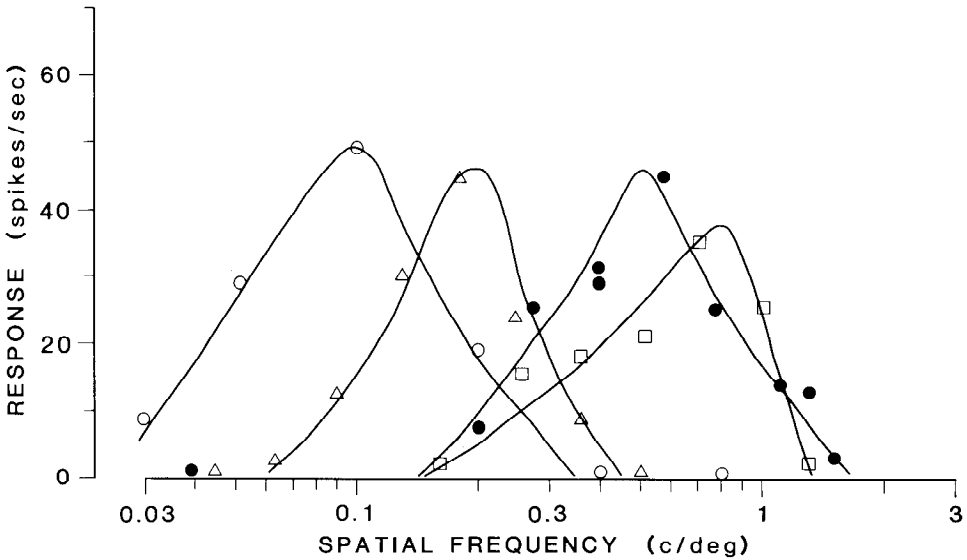


FIG. 5. Response (measured as increased in mean firing rate) for 4 cells as a function of the spatial frequency of the drifting sinusoidal grating. Temporal frequency and the contrast of the gratings were: for *open circles* 7 Hz, 20%; for *open triangles* 10 Hz, 14%; for *filled circles* 4.8 Hz, 10%; for *open squares* 2 Hz, 20%. Index of relative modulation and spontaneous activity (spikes/s) were for *open circle* 1.4 and 1, for *open triangles* 1.5 and 0.7, for *closed circles* 0.04 and 2, for *open squares* 0.06 and 0, respectively.

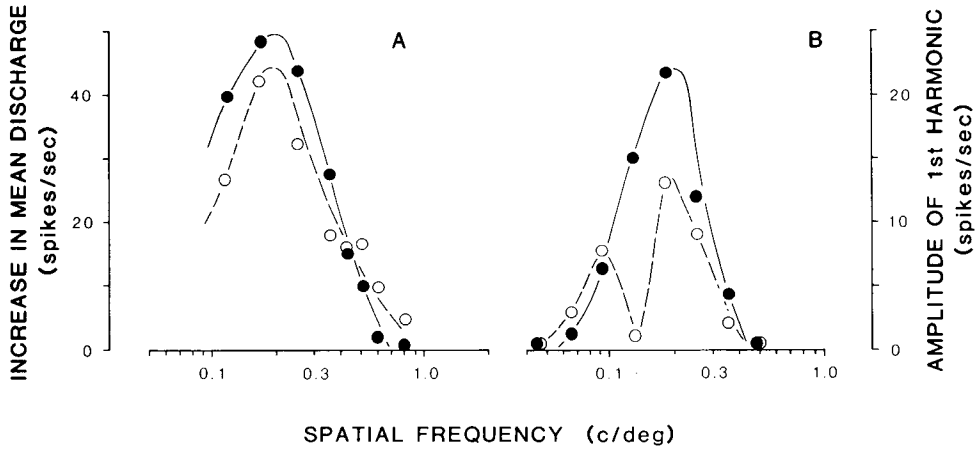


FIG. 6. Amplitude of first harmonic modulation and increase in mean discharge for 2 cells (*A* and *B*) in response to sinusoidal gratings of various spatial frequencies. *Open circles*: show first harmonic amplitude of modulation (*right-hand scale*). *Closed circles*: show the increase in mean discharge (*left-hand scale*). For both cells the stimulus contrast was 15% and the temporal frequency 7 Hz.

6A. However, we cannot exclude completely the possibility that these cells actually had a dip in the modulation tuning curve that was not sampled during our measurements (our sample frequency was usually 0.5 octaves).

Given the discrepancy between the two different tuning curves and the unusual shape of the modulation curve, we chose to use the increase in mean discharge as the primary measure to characterize spatial frequency tuning and other cell properties.

Figure 7*A* shows the distribution of preferred spatial frequencies of all the sampled PMLS cells. They range from 0.1 to 1 cpd and are distributed fairly uniformly over this range. Optimal spatial frequencies of PMLS cells were well correlated with their spatial acuities (the highest spatial frequency that could elicit a response). The higher the preferred spatial frequency of a cell, the higher its acuity, with a correlation coefficient of $r = +0.89$. There was, however, no correlation between preferred spatial frequency and receptive field size of PMLS cells; neither for the cell types that modulate nor for those that do not (see Fig. 8*B*). For all sizes of receptive fields, there was a range of spatial frequency selectivity, with the correlation coefficient between field size and preferred spatial frequency being $r = -0.027$. This is perhaps to be expected as preferred spatial frequency is correlated with acuity, and acuity has been shown to be uncorrelated with receptive field size (23).

In this sense, PMLS cells differ markedly from cells of *areas 17* and *18* of both cat and monkey and also from X- and Y-LGN cells.

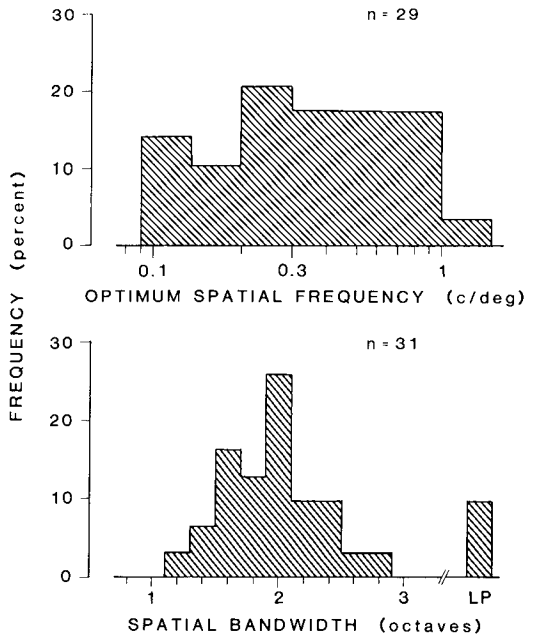


FIG. 7. Frequency distribution of the preferred frequencies and of the bandwidths of spatial tuning curves. Spatial bandwidth is defined as the full width of the tuning curve at half height, expressed as the base 2 logarithm (octaves). LP class represents cells with no low-frequency attenuation. Cells with receptive field center located >30 deg of eccentricity have been excluded from the distributions.

For those cell types, spatial frequency preference (as well as acuity) is well correlated with the size of the cell receptive field (37, 40, 57). Furthermore, in those areas, the product of spatial frequency preference and receptive field size tends to range from 1 to 3 in both cat (40) and monkey (26) [that incidentally agrees well with psychophysical measurements (1)]. In PMLS, however, the product is far from constant (reflecting the lack of correlation) and is on average far higher: the average product is 5, and is as high as 22 in the extreme. For example cell 3 of Fig. 5 (filled circles) has a receptive field that extends $>9^\circ$, yet prefers a grating of spatial frequency 0.5 cpd (i.e., periodicity of 2°). At the optimal stimulation frequency, four and a half periods encompass the field. When the grating period is equal to the receptive field size (spatial frequency of 0.11 cpd), the cell does not respond at all.

Figure 7B shows the distribution of tuning bandwidths for the sampled PMLS cells. They range from one to three octaves and are typically about two octaves. Tuning bandwidth was not significantly correlated with spatial frequency preference ($r = -0.24$). However, there was a strong correlation between spatial tuning bandwidth and receptive field size (see Fig. 8A). Cells with larger receptive fields were

less selective to spatial frequency than those with small receptive fields ($r = +0.89$) and the correlation held for both cells that modulated and those that did not. The implications of this result will be considered in the discussion section.

Contrast

Like cells of other visual areas, PMLS cells respond more strongly to high contrast than to low contrast stimuli. Figure 9 shows the response of four typical PMLS cells to sinusoidal gratings as a function of grating contrast. At moderate contrasts (up to say 10%) the firing rate of all cells increased monotonically (roughly logarithmically) with contrast. At contrasts of >10 times threshold, some cells (75%) saturated, showing uniform or even decreased response to higher contrasts. For this reason and the fact that high contrasts tended to increase the spontaneous discharge of the cell's activity, most of the results were recorded with gratings of $\sim 10\%$ contrast.

Although the thresholds and saturation point of the four cells in Fig. 9 vary somewhat, the slope (before saturation) of all the cells is roughly equal, at 20 spikes/s per log unit contrast. All 12 cells for which we measured contrast response curves had this slope. In this

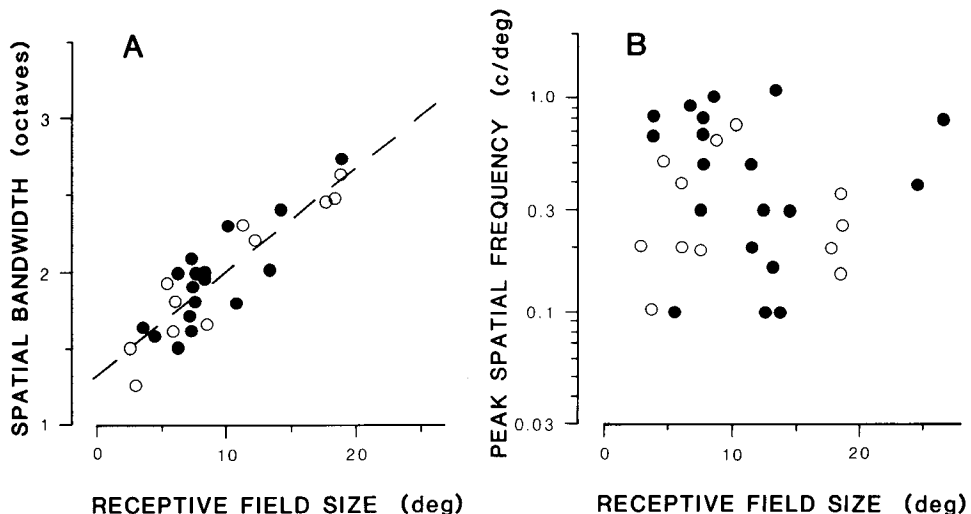


FIG. 8. Scatter diagrams of spatial bandwidth (A) and preferred spatial frequency (B) against cell receptive field size. RF size is expressed as the square root of the area. Dashed lines: show the linear least-square fit. Correlation coefficients were 0.89 for A and 0.03 for B. Open circles: represent cells with index of relative modulation (RMI) > 0.6 . Closed circles: show cells with RMI < 0.6 . No systematic difference between the 2 classes is apparent. Cells with receptive field centers of >30 deg of eccentricity were excluded.

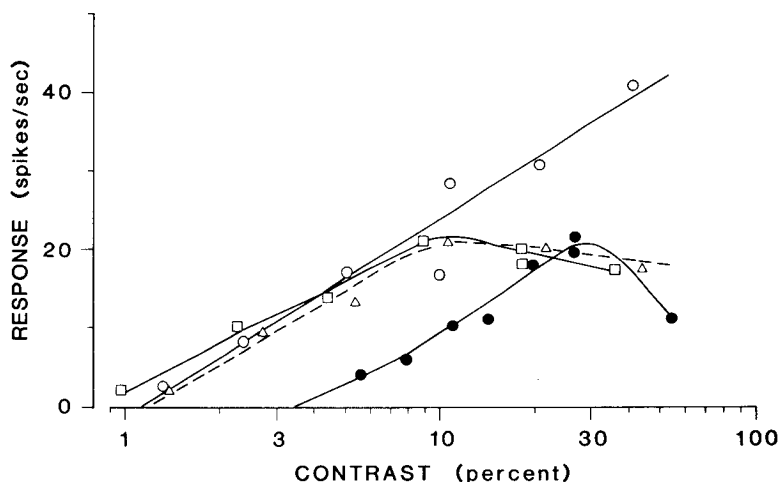


FIG. 9. Response of 4 cells as a function of the contrast of a drifting sinusoidal grating. *Open circles*: spatial frequency 0.3 cpd, temporal frequency 4 Hz, cell spontaneous activity 10 spikes/s, index of relative modulation. (RMI) 0.73. *Open squares*: spatial frequency 0.08 cpd, temporal frequency 5 Hz, cell spontaneous activity 2 spikes/s, RMI 0.05. *Open triangles*: spatial frequency 0.9 cpd, temporal frequency 6 Hz, RMI 0.9. *Filled circles*: spatial frequency 0.6 cpd, temporal frequency 5 Hz, spontaneous activity 3 spikes/s, RMI 0.65. Note that for this cell the spatial frequency of the grating was nonoptimal and near acuity, explaining the higher threshold.

respect, PMLS cells behave differently from most other visual areas (such as LGN, *areas 17 and 18*, and colliculus), where the contrast gain varies considerably and depends critically on the stimulus (5, 11, 20, 39).

Temporal frequency selectivity

When a grating is caused to drift, the rate at which its bars move past a particular point is its temporal frequency, which is directly proportional to both the spatial frequency and drift velocity of the grating ($TF = SFv$). In the next sections we report measurements of both temporal frequency and velocity selectivity.

Figure 10 shows the response of four representative cells as the temporal frequency of the drifting grating is varied. These cells all responded selectively to stimuli within an appropriate temporal frequency range. Frequencies too high or too low are ineffective in eliciting a strong response, implying band-pass temporal tuning.

Figure 11 shows the distributions of preferred temporal frequency for PMLS cells, together with their bandwidths. All cells prefer temporal frequencies from ~2 to 10 Hz, with bandwidths of ~2 octaves (roughly equivalent to the spatial bandwidths described earlier). The bandwidths are quite small in comparison with other areas, particularly *area 17*, where

the majority of cells have no low-temporal frequency attenuation (10, 46, 63).

Spatiotemporal coupling

The curves of Fig. 10, and all the results of Fig. 11, were measured with gratings of optimal spatial frequency. Similarly, the spatial frequency tuning results of Figs. 5 and 6 were measured at optimal temporal frequencies. An interesting question is whether the spatial selectivity depends on the temporal frequency of the stimulus and the temporal selectivity on the spatial frequency of the stimulus. In *area 17*, the spatial and temporal properties are independent (10, 63), whereas in *area 18*, the preferred spatial frequency varies inversely with the temporal frequency of the test grating and vice versa (10).

Figure 12 reports tuning curves measured at various spatial and temporal frequencies. On the left are plotted spatial tuning curves measured with gratings of various temporal frequencies, and on the right temporal frequency tuning curves measured at various spatial frequencies. There were two general types of cell response: some were spatiotemporally coupled and others not. A representative cell of each class is reported.

Cell *A* has similar spatial frequency tuning curves for all temporal frequencies. They de-

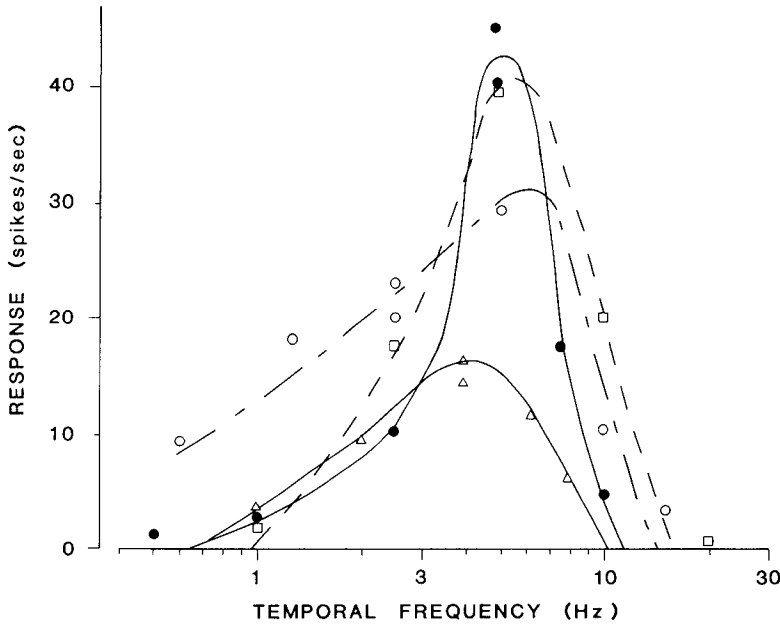


FIG. 10. Temporal frequency tuning curves for stimulation by drifting sinusoidal gratings, for 4 representative cells. Grating spatial frequencies were optimal for each cell. Spatial frequencies and contrasts were: for *open squares* 0.08 cpd and 40%; for *open circles* 0.2 cpd and 10%; for *open triangles* 0.5 cpd and 30%; for *filled circles* 0.1 cpd and 7%. Index of relative modulation and spontaneous discharge were: for *open squares* 0.02 and 13 spikes/s; for *open circles* 1 and 1 spikes/s; for *open triangles* 0.15 and 3.6 spikes/s; for *filled circles* 0.09 and 15 spikes/s.

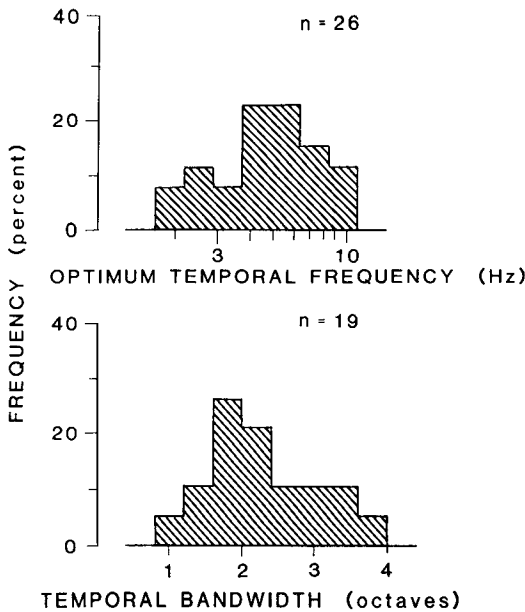


FIG. 11. Frequency distributions of optimum temporal frequency and of temporal bandwidth. Bandwidth is defined as full width at half height. Only cells whose receptive fields were within 30 deg from area centralis have been included in the distributions.

crease uniformly as the temporal frequency becomes less optimal, but there is no shift in the peak nor in the width. That is to say, spatial frequency preference is independent of temporal frequency. Similarly, the temporal frequency tuning curves do not change in peak frequency or width with varying spatial frequency. For cell *B*, however, as the temporal frequency was varied from the optimal, not only did the response level of the cell decrease, but the preferred spatial frequency changed. The higher the temporal frequency, the lower the preferred spatial frequency. Similarly, for temporal tuning, the higher the spatial frequency, the lower the preferred temporal frequency.

Unfortunately we have complete spatio-temporal data on only six cells. Of these, three behaved like cell *A* of Fig. 12, and three like cell *B*, showing spatiotemporal coupling. Of our small sample, half were like *area 17* and half like *area 18* cells. The three spatiotemporally coupled cells had relative modulation indexes of 0.1, 0.5, and 1 and the spatiotemporally uncoupled cells 0.04, 0.06, and 1.3.

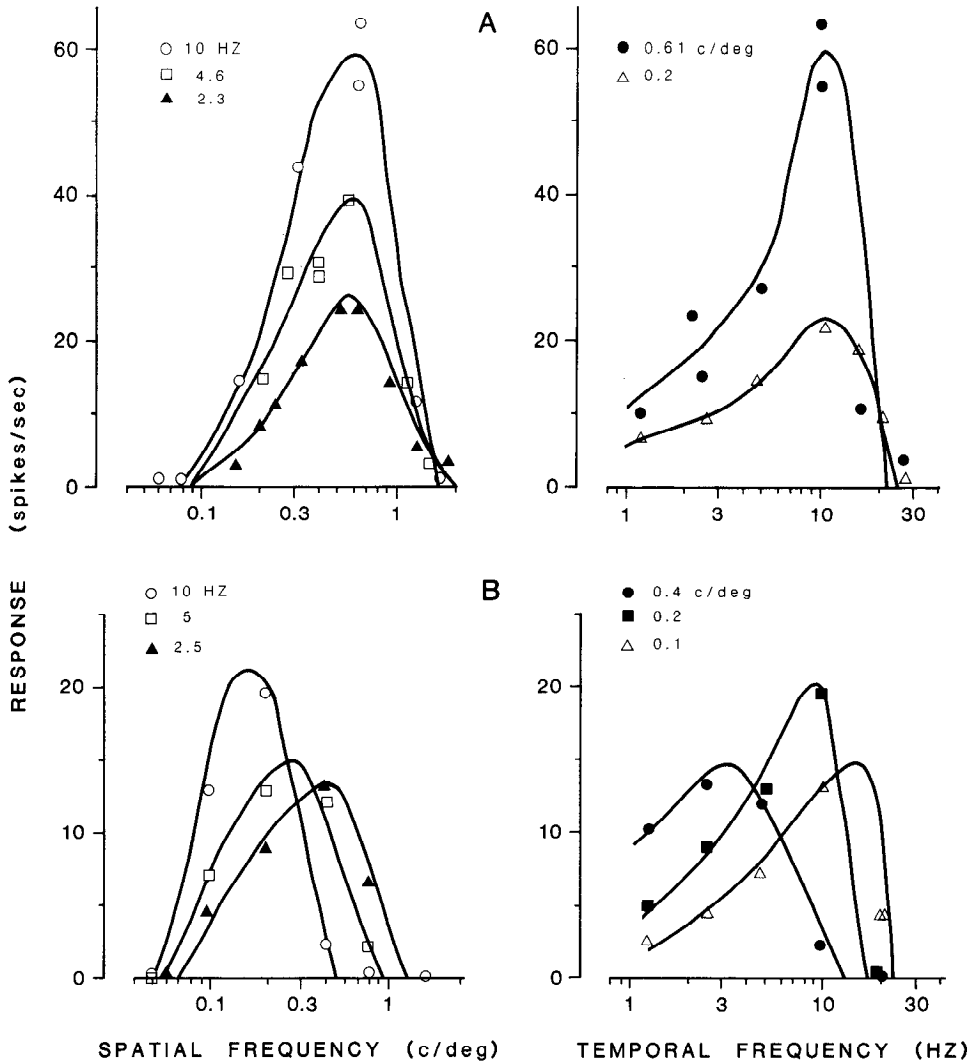


FIG. 12. Spatial frequency (left column) and temporal frequency (right column) tuning curves for 2 different cells (A and B) at various temporal (left) and spatial (right) frequencies. Grating contrast was 30% for A and 10% for B. Two cells were recorded from the same penetration and were only 200 μm apart. Cells A and B had a spontaneous activity of 8 and 2.7 spikes/s and an index of relative modulation of 0.04 and 0.1, respectively.

There was no link between spatiotemporal coupling and cells type.

Velocity selectivity

Selectivity to velocity is known to be broad for most PMLS cells (15, 58, 66). In Fig. 13 (bottom curve) we show the velocity tuning curve of a PMLS cell to stimulation by a bar. As Spear and Bauman (58) observed, selectivity is broad. Velocities between 15 and 300 deg/s elicit a response greater than half the maximum, implying a bandwidth of 4.3 oc-

taves. However, when the same cell is stimulated by sinusoidal gratings (upper curves), the velocity tuning curves are much sharper, more in the region of two octaves (Fig. 13).

To understand this result one must appreciate the relationship between velocity, temporal frequency, and spatial frequency: $v = \text{TF}/\text{SF}$. For a fixed single spatial frequency, velocity is proportional to temporal frequency. Velocity tuning will therefore reflect temporal frequency tuning. As the spatial frequency of the stimulus is changed, the constant of pro-

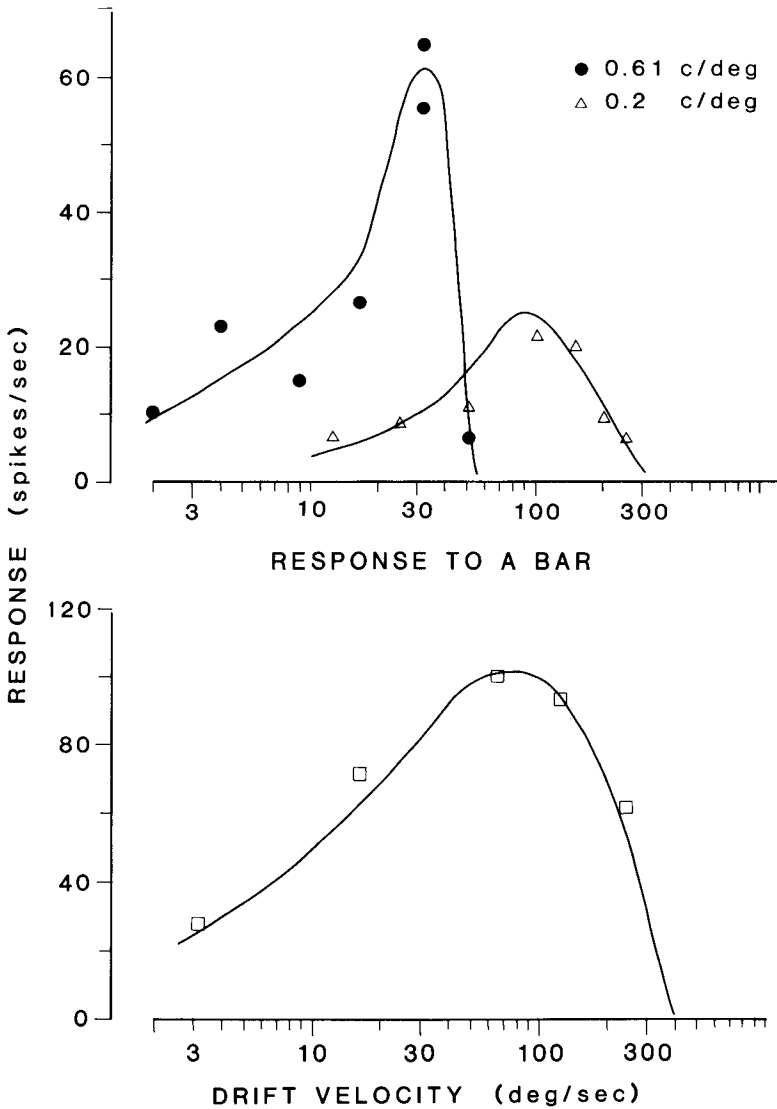


FIG. 13. Response of a cell to 2 sinusoidal gratings (0.61 and 0.2 cpd; *top*) and to a black bar (of 2 deg width; *bottom*), as a function of drift velocity. Grating contrast was 30%. Response to the bar is defined as the difference between the maximum and the spontaneous activity, whereas that for the grating is the difference between mean and spontaneous activity.

portionality will change. Velocity tuning will still reflect temporal frequency tuning, but the whole tuning curve will be multiplied by a different constant. On a logarithmic scale multiplication corresponds to a horizontal displacement. The peaks of the two upper curves of Fig. 13 are displaced by a factor of three, corresponding to the ratio of stimulus spatial frequencies.

A bar comprises not a single spatial frequency, but many. Thus the velocity tuning

profile generated by a bar may be expected to embrace all the tuning curves of sinusoids of different frequencies. Therefore, it may be expected to be much broader than that for a single sinusoidal grating.

The cell of Fig. 13 was one of the type that was not spatiotemporally coupled (like cell *A* of Fig. 12). Cells that were spatiotemporally coupled showed an even greater shift in velocity peaks with spatial frequency and even broader velocity tuning to stimulation by a

bar. This is because for these cells, preferred temporal frequency varied inversely with spatial frequency, so the change in velocity preference for different spatial frequencies was even greater than if temporal preference remained constant.

Eccentricity

Figure 14 shows how the spatial and temporal frequency preference for the cells in our

sample varied with eccentricity from the area centralis. As may be expected, optimal spatial frequency decreases with increasing eccentricity, as does spatial acuity (23). The average rate of decrease is 0.053 octaves/deg of eccentricity. This agrees qualitatively with results in all other visual structures, including retina. Quantitatively, the decrease is less than *area 17* or *18* (46).

What is perhaps more surprising is that op-

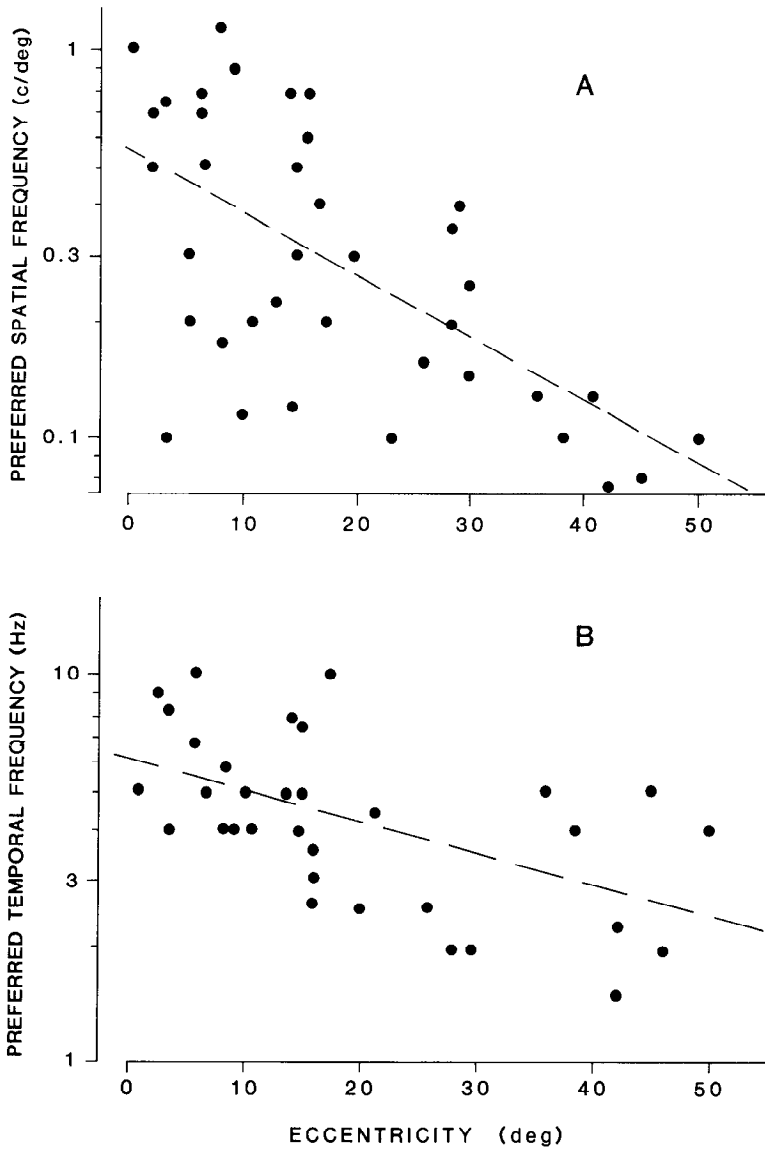


FIG. 14. Scatter diagrams of preferred spatial (A) and temporal (B) frequency against the eccentricity of the cell receptive field center. Lines are the linear least-square fits and have a slope of -0.053 octaves/deg for A ($r = -0.65$) and -0.025 octaves/deg for B ($r = -0.60$).

timal temporal frequency also decreases with eccentricity. At first glance this may seem to contradict the findings that more peripheral cells prefer high velocities (27, 48). However, it should be noted that the rate of decrease in temporal frequency preference is only 0.025 octaves/deg, half that for spatial frequency preference. Thus the higher velocity preference of peripheral cells results from their lower spatial frequency tuning, not from higher temporal tuning.

DISCUSSION

Pattern of response

Many investigators (15, 29, 33, 56, 58) have noted that although a few PMLS cells have receptive fields divided into distinct ON and OFF regions, the majority have an ON/OFF organization, with homogeneous response to both ON and OFF stimuli placed anywhere within their receptive fields. We confirm this general observation, and report further data consistent with the existence of two general receptive field types.

Cells with ON/OFF receptive fields responses gave a characteristic response to drifting bars and gratings and to flickering gratings. Drifting bars elicited an overall increase in firing rate, with no modulation. Drifting gratings similarly produced an unmodulated increase in firing rate, and flickering gratings caused second harmonic modulation, with no accompanying first harmonic modulation at any spatial phase. This pattern of response is very similar to that of complex cells in *areas 17* and *18* of both cat (39, 45, 59) and monkey (22, 26, 53).

Cells that showed some indication of separate ON and OFF regions responded differently to all three stimuli: there was some response modulation to drifting bars, a stronger modulation to drifting gratings (RMIs > 0.8), and for flickering gratings of appropriate phase there was a strong first harmonic modulation. There was, however, no clear null point, and some second harmonic modulation was always present. These cells are not quite like classical simple cells for several reasons. Simple cells behave in a quasilinear fashion in response to flickering stimuli (39, 44, 59). Simple cells in monkey (22) and cat (21) have a relative modulation index > 1 with a distribution peaking ~1.5; only two cells in our sample had RMI > 1.4. For classical simple cells the

spatial frequency tuning curve measured as the first harmonic modulation is similar in form to that measured as the increase in discharge, presumably reflecting the half-wave rectification (44). For PMLS cells that modulate to drifting gratings, the tuning curves of the first harmonic component are often of different form from those of the average discharge (see Fig. 6).

Pollen and his co-workers (25, 50, 51) have observed a subclass of complex cells, called periodical complex cells, that modulate to drifting gratings and bars. The spatial frequency tuning curves of the modulation component of periodic complex cells is double peaked, whereas that of the mean discharge is typically single peaked (50). Dean and Tolhurst (21) described a subclass of complex cells on the basis of the discreteness of subregions of the receptive field. Epstein and Hochstein (59, 60) classified complex cells as mixed or intermediate if they responded to flickering gratings with mainly second harmonic modulation but showed first harmonic modulation at some spatial phases. The characteristic of periodical, mixed, or intermediate complex cells, and of those with high discreteness are all very similar to the class of PMLS cells with high relative modulation index. We shall refer to them as mixed complex cells.

In practice not every cell could be neatly categorized into complex or mixed class on the basis of discreteness of receptive field subregions or on the basis of its response patterning to gratings. As in the primary visual cortex, many cells showed a weak modulation superimposed on a pedestal of general firing increase and these cells had intermediate modulation index. However, with this reservation, it is interesting to note that in all cortical areas studied to date, there exist, both in felines and primates, cells of both of the above two classes: one responding with a modulation of firing rate (pseudolinearity) and the other with an overall increase in activity (22, 26, 39, 41, 44, 45, 53). It is possible that the two cell classes have separate roles in vision and encode different aspects of visual information (19).

Contrast sensitivity

The response of PMLS cells, like that of cells of all other visual structures (5, 11, 39, 61), increases monotonically with increasing stimulus contrast up to the point of saturation. The

minimal (threshold) contrast to elicit a response of PMLS cells is quite low ($\sim 1\%$), similar to that for *area 17* and *18* cells and also for X- and Y-geniculate cells. However, superior colliculus and geniculate W-cells, both of which form major direct and indirect inputs to PMLS, have much higher thresholds, $\sim 10\%$ (11, 61). Therefore, at low stimulus contrasts, superior colliculus and W-geniculate cells should not influence cell behavior.

The majority of PMLS cells tended to saturate at moderate contrasts ($\sim 10\%$) when stimulated by the preferred stimulus. This is low compared with *areas 17* and *18* cells, where responses increase monotonically up to $\sim 30\%$. Possibly the influence of the high-threshold input of superior colliculus (via pulvinar) and W-cells at about this contrast causes the saturation.

Spatial properties

Although PMLS cells are heterogeneous in many respects, including their spatial properties [Camarada and Rizzolatti (15) report 5 classes based on spatial summation tests], it is interesting that nearly all the cells in our sample were selective for spatial frequency. The preferred spatial periodicity of all the cells we studied was considerably smaller than the size of the receptive fields. This agrees with previous reports (33, 58) that cells respond to objects much smaller than their receptive fields.

In the primary visual areas, the size of the receptive field determines the spatial frequency preference of the cell, especially for simple cells (22, 40): the larger the field, the lower the preferred spatial frequency. This results from the fact that the majority of receptive fields of a given cell type differ principally by a scaling factor, which determines both the field size and preferred spatial frequency. However, with PMLS cells, there is no such relationship. The spatial frequency preference is completely independent of receptive field size and much higher than the size would suggest.

A strong positive correlation was observed between receptive field size and selectivity bandwidth (expressed in octaves of full width at half height). The smaller the field, the finer the selectivity. One possible explanation for the observed correlation is that each PMLS neuron was multiple inputs (possibly from several visual areas) that do not overlap exactly in space, creating large receptive fields. If these

inputs vary slightly in their spatial frequency selectivity, the combined selectivity will be broader than each of the inputs. A greater number of inputs means a larger receptive field and broader tuning, accounting for the positive correlation. This suggests that much of the observed tuning derives directly from the afferents, but does not preclude the possibility that further spatial frequency selectivity is achieved by local circuitry.

It is worthwhile noting that for both classical and mixed complex cells the receptive field size is independent of spatial frequency preference but is correlated with the selectivity bandwidth. For both types of cells the RF size and the bandwidth could result from the excitation of multiple input or subunits as previously described. The different type of non-linearity could derive from a different spatial overlap of the subunits, as Epstein and Hochstein (59, 60) suggest for *area 17* complex cells. Their model of the complex RF is based on linear subunits with different spatial overlap and a nonlinear summation stage between subunits. There is at present no evidence at strong linear input to PMLS, with the exception perhaps of few simple cells, or linear W cells (31). However, many of the properties of PMLS cells could be reproduced using nonlinear subunits of the type of Y-cells, that form a major input to PMLS (6).

Another and perhaps more simple explanation for the two types of nonlinear behavior could be that the nonlinearity derives directly from the cortical input, mainly complex cells (31), and the input cells themselves already exhibit the nonlinearity.

The distribution of the preferred spatial frequency in PMLS cells is interesting. The range is between 0.1 and 1 cpd, similar to that reported for cortical *area 18* (4, 46) and for superior colliculus (11), and about a factor of two lower than that for *area 17* (4, 40, 46). The distribution of frequency preference is much flatter in PMLS than in other areas, which are normally peaked around a central value. Thus PMLS has a relatively higher representation of cells preferring very low spatial frequencies.

Temporal properties

All PMLS cells that we studied were selective for temporal frequency. The peak was always ~ 4 – 10 Hz and all showed a heavy at-

tenuation for low as well as for high temporal frequencies (bandpass). This contrasts with *area 17*, where all cells respond well to very low temporal frequencies (lowpass) (10, 46, 63). It is interesting that PMLS cells do not respond to low temporal frequencies, given the heavy *area 17* projection. One possibility is that the indirect influence from superior colliculus inhibits the low temporal frequency response. This would agree with Smith and Spear's (56) observation that PMLS cells respond to lower velocities after collicular ablation.

Previous studies report a wide variation of velocity preference for PMLS cells and that individual cells respond to a wide range of velocities (15, 58, 66). Our results show that the range of velocity preferences for PMLS cells result from a variation in spatial frequency selectivity rather than a variation in temporal frequency, or velocity selectivity. The response of individual cells to a wide range of velocities can be readily explained by considering the Fourier spectra of the bars or spots commonly used as stimuli. These stimuli comprise a large range of spatial frequency components. Each of the component frequencies (within the tuning range of the cell) can elicit independently a response and will do so when the component frequencies are modulated at appropriate temporal frequency. As temporal frequency is equal to the product of spatial frequency and velocity, the optimal velocity for the low spatial frequencies will be higher than for the high spatial frequency components. Thus, by stimulation with a broad spectrum stimulus like a bar, we expect a broad velocity tuning.

For six cells we investigated in detail the spatial and temporal responses. For three of these cells, the spatial properties were not dependent of the temporal tuning (spatiotemporally uncoupled) and for the other three the spatial and temporal properties were coupled: the higher the temporal frequency, the lower the spatial preference, and vice versa. The coupled cells were like those of *area 18* (10) and the uncoupled like those of *area 17* (10, 63). The coupling could therefore simply reflect the input properties of PMLS cells. In *area 17* and *18* spatiotemporal coupling does not vary between simple-like and complex-like cells. Similarly, in PMLS there is no distinction on the basis of cell classification.

Note that this spatiotemporal coupling does not lead to velocity tuning, as the correlation

is negative. For constant velocity tuning, spatial and temporal preference should be positively correlated ($v = TF/SF$), as Newsome et al. (47) observe for some cells of monkey area MT. The functional role of the PMLS coupling is not clear and may simply reflect the structure of PMLS cells and their inputs. Alternatively, it may assist in maintaining velocity constancy with varying viewing distance. We found no evidence for cells being tuned for velocity: velocity tuning was simply a consequence of their spatial and temporal frequency characteristics. This agrees with measurements in other visual areas (26) and also with psychophysical measurements in man (2).

Concluding remarks

The high selectivity for spatial and temporal frequency is surprising, given the lack of selectivity for spatial localization, orientation, and velocity. Although there is not a great deal of evidence at this stage, it is worth speculating on the functional significance of the properties of PMLS cells.

One possibility is that the area is involved with stereopsis, particularly for motion in depth. Most PMLS cells are binocular and many cannot be driven by one eye alone (65, 67). They respond well to changing disparity, which occurs with movement towards or away from the animal. Large receptive fields would be an obvious advantage for this type of analysis, as a single cell could track an object for a considerable time, which is necessary for any disparity matching system. Orientation specificity is not required for this task, but as Marr and Poggio (42) have demonstrated, spatial frequency selectivity can be advantageous in solving the binocular matching problem.

Another possibility difficult to exclude is that the LS area is involved in motion perception. In human vision, motion detectors extend over a wide range of spatial frequencies, down to 0.03 cpd (1, 2, 13), but do not seem to be prevalent at high spatial frequencies (17, 18, 36, 68). All motion detectors seem to be finely tuned for temporal and spatial frequency (2) the narrow tuning aiding in velocity detection and in analysis of the object in motion (12, 14). With the obvious reservations in passing from psychophysics to single unit physiology and from one species to another, we suggest that characteristics of PMLS neurons, with the high representation of low spatial frequencies and the relatively narrow spa-

tial and temporal selectivity, make them likely candidates for some of the tasks involved in motion perception.

ACKNOWLEDGMENTS

We thank Peter Meyer, Tony Gibbs, Alex Wilkie, David Ray, and Keith Leppard for expert technical assistance and John Ross for support and helpful discussions. We also thank an anonymous referee for his thorough reading and criticism of the manuscript. M. Di Stefano was on leave

from the University of Pisa and M. C. Morrone from the Scuola Normale Superiore, Pisa. D. Burr received a QEII Fellowship from the Australian Department of Science, and the Australian National Health and Medical Research Council provided partial support for the project. Hydron Australia donated the contact lenses.

Present address of M. Di Stefano: Istituto di fisiologia umana, Via S. Zeno 35, Pisa, Italy.

Received 25 March 1985; accepted in final form 1 May 1986.

REFERENCES

- ANDERSON, S. J. AND BURR, D. C. Receptive field size of human motion detection units. *Vision Res.* In press.
- ANDERSON, S. J. AND BURR, D. C. Spatial and temporal selectivity of the human motion detection system. *Vision Res.* 25: 1147-1154, 1985a.
- ANDREWS, B. W. AND POLLEN, D. A. Relationship between spatial frequency selectivity and receptive field profile of simple cells. *J. Physiol. Lond.* 287: 163-176, 1979.
- BERARDI, N., BISTI, S., FIORENTINI, A., AND MAFFEI, L. Correlation between the preferred orientation and spatial frequency of neurones in visual areas 17 and 18 of the cat. *J. Physiol. Lond.* 233: 603-618, 1982.
- BERARDI, N. AND MORRONE, M. C. The role of γ -aminobutyric acid mediated inhibition in the response properties of cat lateral geniculate nucleus neurones. *J. Physiol. Lond.* 357: 505-523, 1984.
- BERSON, D. M. Cat lateral suprasylvian cortex: Y-cell inputs and corticocortical projections. *J. Neurophysiol.* 53: 544-556, 1985.
- BERSON, D. M. AND GRAYBIEL, A. M. Parallel thalamic zones in the LP-pulvinar complex of the cat identified by their afferent and efferent connections. *Brain Res.* 147: 139-148, 1978.
- BERSON, D. M. AND GRAYBIEL, A. M. Subsystems within the visual association cortex as delineated by their thalamic and transcortical affiliations. In: *Vision, Brain, and Cooperative Computation*, edited by M. Arbib and A. Hanson. Cambridge, MA: MIT Press. In press.
- BISHOP, P. O., KOZAK, W., AND VAKKUR, G. J. Some quantitative aspects of the cat's eye: axis and plane of reference, visual field coordinates and optics. *J. Physiol. Lond.* 163: 465-502, 1962.
- BISTI, S., CARMIGNOTTO, G., GALLI, L., AND MAFFEI, L. Spatial frequency characteristics of neurons of area 18 in the cat: dependence on the velocity of the visual stimulus. *J. Physiol. Lond.* 359: 259-268, 1985.
- BISTI, S. AND SIRETENU, L. Sensitivity to spatial frequency and contrast of visual cells in cat superior colliculus. *Vision Res.* 16: 247-251, 1976.
- BURR, D. C. AND ROSS, J. Visual processing of motion. *Trends in Neurosci.* 9: 304-307, 1986.
- BURR, D. C. AND ROSS, J. Contrast sensitivity at high velocities. *Vision Res.* 23: 3567-3569, 1982.
- BURR, D. C., ROSS, J., AND MORRONE, M. C. Seeing objects in motion. *Proc. Roy. Soc. Lond.* B227, 249-265, 1986.
- CAMARDA, R. AND RIZZOLATTI, G. Visual receptive fields in the lateral suprasylvian area (Clare-Bishop area) of the cat. *Brain Res.* 101: 427-443, 1976.
- CAMPBELL, F. W., COOPER, G. F., AND ENROTH-CUGELL. The spatial selectivity of the visual cells of the cat. *J. Physiol. Lond.* 203: 223-235, 1969.
- CAMPBELL, F. W. AND MAFFEI, L. Stopped visual motion. *Nature Lond.* 278: 55, 1979.
- CAMPBELL, F. W. AND MAFFEI, L. The influence of spatial frequency and contrast on the perception of moving patterns. *Vision Res.* 21: 713-721, 1981.
- CATTANEO, A., MAFFEI, L., AND MORRONE, M. C. Patterns in the discharge of simple and complex visual cortical cells. *Proc. Roc. Soc. Lond. B* 212: 279-297, 1981.
- DEAN, A. F. The relationship between response amplitude and contrast for cat striate cortical neurones. *J. Physiol. Lond.* 318: 413-427, 1981.
- DEAN, A. F. AND TOLHURST, D. J. On the distinctness of simple and complex cells in the visual cortex of the cat. *J. Physiol. Lond.* 344: 305-325, 1983.
- DE VALOIS, R. L., ALBRECHT, D. G., AND THORELL, L. G. Spatial frequency selectivity of cells in macaque visual cortex. *Vision Res.* 22: 545-559, 1982.
- DI STEFANO, M., MORRONE, M. C., AND BURR, D. C. Visual acuity of neurones in the cat lateral suprasylvian cortex. *Brain Res.* 331: 382-385, 1985.
- ENROTH-CUGELL, C. AND ROBSON, J. The contrast sensitivity of retinal ganglion cells of the cat. *J. Physiol. Lond.* 187: 517-522, 1966.
- FELDON, S. E., ANDREWS, B. W., AND POLLEN, D. A. Periodic complex cells in cortical area 19 of the cat. *Vision Res.* 18: 347-350, 1978.
- FOSTER, K. H., GASKA, J. P., NAGLER, M., AND POLLEN, D. A. Spatial and temporal frequency selectivity of neurones in visual cortical areas V1 and V2 of the macaque Monkey. *J. Physiol. Lond.* 365: 331-336, 1985.
- FRISHMAN, L. O., SCHWEITZER-TONG, D. E., AND GOLDSTEIN, E. B. Velocity tuning of cells in dorsal lateral geniculate nucleus and retina of the cat. *J. Neurophysiol.* 50: 1393-1414, 1983.
- HAMMOND, P. Inadequacy of nitrous oxide/oxygen for maintaining anaesthesia in cats: satisfactory alternatives. *Pain* 5: 143-152, 1978.
- HARUTIVNIAN-KOZAK, B. A., DJAVADIAN, R. L., AND MELKUMIAN, A. V. Responses of neurones in cat's Lateral Suprasylvian area to moving light and dark stimuli. *Vision Res.* 24: 189-195, 1984.
- HEATH, C. J. AND JONES, E. G. The anatomical organization of the suprasylvian gyrus of the cat. *Ergeb. Anat. Entwicklungsgesch.* 45: 1-64, 1971.
- HENRY, G. H., LUND, J. B., AND HARVEY, A. R. Cells of the striate cortex projecting to the Clare-Bishop area of the cat. *Brain Res.* 151: 154-158, 1978.

32. HOCHSTEIN, S. AND SHAPLEY, R. M. Quantitative analysis of retinal ganglion cell classifications. *J. Physiol. Lond.* 262: 237–264, 1976.
33. HUBEL, D. H. AND WIESEL, T. N. Visual area of the lateral suprasylvian gyrus (Clare-Bishop area) of the cat. *J. Physiol. Lond.* 202: 251–260, 1969.
34. HUGHES, A. A supplement of the cat schematic eye. *Vision Res.* 16: 149–154, 1976.
35. HUGHES, H. C. Efferent organization of the cat pulvinar complex with a note on bilateral claustric and reticulo cortical connections. *J. Comp. Neurol.* 193: 937–963, 1980.
36. KULIKOWSKI, J. J. AND TOLHURST, D. J. Psychophysical evidence for sustained and transient neurones in the human visual system. *J. Physiol. Lond.* 232: 149–162, 1973.
37. LEHMKUHL, S., KRATZ, K. E., MANGEL, S. C., AND SHERMAN, S. M. Spatial and temporal sensitivity of X- and Y-cells in dorsal lateral geniculate nucleus of the cat. *J. Neurophysiol.* 43: 520–541, 1980.
38. LEVENTAL, A. G., KEENS, T., AND TORK, I. The afferent ganglion cells and cortical projections of the retina recipient zone (RRZ) of the cat's "pulvinar complex." *J. Comp. Neurol.* 194: 535–554, 1980.
39. MAFFEI, L. AND FIORENTINI, A. The visual cortex as a spatial frequency analyzer. *Vision Res.* 13: 1255–1267, 1973.
40. MAFFEI, L. AND FIORENTINI, A. Spatial frequency rows in the striate visual cortex. *Vision Res.* 17: 257–264, 1977.
41. MAFFEI, L., MORRONE, M. C., PIRCHIO, M., AND SANDINI, G. Response of visual cortical cells to periodic and non-periodic stimuli. *J. Physiol. Lond.* 296: 27–47, 1979.
42. MARR, D. AND POGGIO, T. A computational theory of human stereo vision. *Proc. R. Soc. Lond. B Biol. Sci.* 204: 301–328, 1979.
43. MARZI, C. A., ANTONINI, A., DI STEFANO, M., AND LEGG, C. R. The contribution of the corpus callosum to receptive fields in the LSA of the cat. *Behav. Brain Res.* 4: 155–176, 1982.
44. MOVSHON, J. A., THOMPSON, I. D., AND TOLHURST, D. J. Spatial summation in the receptive fields of simple cells in the cat's striate cortex. *J. Physiol. Lond.* 283: 53–77, 1978.
45. MOVSHON, J. A., THOMPSON, I. D., AND TOLHURST, D. J. Receptive field organization of complex cells in the cat's striate cortex. *J. Physiol. Lond.* 283: 79–99, 1978.
46. MOVSHON, J. A., THOMPSON, I. D., AND TOLHURST, D. J. Spatial and temporal contrast sensitivity of neurones in area 17 and 18 of the cat's visual cortex. *J. Physiol. Lond.* 283: 101–120, 1978.
47. NEWSOME, W. T., GIZZI, M. S., AND MOVSHON, J. A. Spatial and temporal properties of neurones in macaque MT. *Invest. Ophthalmol.* 24: 106, 1983.
48. ORBAN, G. A., KENNEDY, H., AND MAES, H. Response to movement of neurones in area 17 and 18 of the cat: velocity sensitivity. *J. Neurophysiol.* 45: 1043–1058, 1981.
49. PALMER, L. A., ROSENQUIST, A. C., AND TUSA, R. J. The retinotopic organization of lateral suprasylvian visual areas in the cat. *J. Comp. Neurol.* 177: 237–256, 1978.
50. POLLEN, D. A., ANDREWS, B. W., AND FELDON, S. E. Spatial frequency selectivity of periodic complex cells in the visual cortex of the cat. *Vision Res.* 18: 665–682, 1978.
51. POLLEN, D. A. AND RÖNNER, S. F. Periodic excitability changes across the receptive fields of complex cells in the striate and parastriate cortex of the cat. *J. Physiol. Lond.* 245: 667–697, 1975.
52. RACZKOWSKI, D. AND ROSENQUIST, A. C. Connections of the parvocellular laminae of the dorsal lateral geniculate nucleus with the visual cortex in the cat. *Brain Res.* 199: 447–451, 1980.
53. SCHILLER, P. H., FINLAY, B. L., AND VOLMAN, S. Quantitative studies of single cell properties in monkey striate cortex. III. Spatial frequency. *J. Neurophysiol.* 39: 1334–1351, 1976.
54. SEGRAVES, M. A. AND ROSENQUIST, A. C. The distribution of the cells of origin of callosal projections in cat visual cortex. *J. Neurosci.* 2: 1079–1089, 1982.
55. SHAPLEY, R. AND HOCHSTEIN, S. Visual spatial summation in two classes of geniculate cells. *Nature Lond.* 256: 411–413, 1975.
56. SMITH, D. C. AND SPEAR, P. D. Effects of superior colliculus removal of receptive-field properties of neurons in lateral suprasylvian visual area of the cat. *J. Neurophysiol.* 42: 57–75, 1979.
57. SO, Y. T. AND SHAPLEY, R. Spatial tuning of cells in and around lateral geniculate nucleus of the cat: X and Y relay cells and perigeniculate interneurons. *J. Neurophysiol.* 45: 107–120, 1981.
58. SPEAR, D. AND BAUMANN, T. P. Receptive-field characteristics of single neurons in lateral suprasylvian visual area of the cat. *J. Neurophysiol.* 38: 1403–1420, 1975.
59. SPITZER, H. AND HOCHSTEIN, S. Simple- and complex-cell response dependences on stimulus parameters. *J. Neurophysiol.* 53: 1244–1265, 1985.
60. SPITZER, H. AND HOCHSTEIN, S. A complex-cell receptive field model. *J. Neurophysiol.* 53: 1266–1286, 1985.
61. SUR, M. AND SHERMAN, S. M. Linear and nonlinear W-cells in C-laminae of the cat's lateral geniculate nucleus. *J. Neurophysiol.* 47: 869–884, 1982.
62. SYMONDS, L. L. AND ROSENQUIST, A. C. Projections of the pulvinar-lateral posterior complex to visual cortical areas in the cat. *Neuroscience* 6: 1995–2020, 1981.
63. TOLHURST, D. J. AND MOVSHON, J. A. Spatial and temporal contrast sensitivity of striate cortical neurones. *Nature Lond.* 257: 674–675, 1975.
64. TONG, L., KALIL, R. E., AND SPEAR, P. D. Thalamic projections to visual areas of the middle suprasylvian sulcus in the cat. *J. Comp. Neurol.* 212: 103–117, 1982.
65. TOYAMA, K. AND KOZASA, T. Responses of Clare-Bishop neurones to three dimensional movement of a light stimulus. *Vision Res.* 22: 571–574, 1982.
66. TURLEJSKI, K. Visual responses of neurones in the Clare-Bishop area of the cat. *Acta Neurobiol.* 35: 189–208, 1975.
67. VON GRUNAU, M. W., POULIN, C., AND RAUSCHHECKER, J. P. Binocular facilitation in lateral suprasylvian visual area of normal and strabismic cats. *Proc. Int. Union Physiol. Sci.* 15: 1983.
68. WATSON, A. B., THOMPSON, P. G., MURPHY, B. J., AND NACHMIAS, J. Summation and discrimination of gratings moving in opposite directions. *Vision Res.* 20: 341–347, 1980.
69. WRIGHT, M. J. Visual receptive fields of cells in a cortical area remote from the striate cortex in the cat. *Nature Lond.* 223: 973–975, 1969.